Polystyrene nanoplastics are unlikely to aggregate in freshwater bodies

Pirade, Februriyana; Foppen, Jan Willem; van der Hoek, Jan Peter; Lompe, Kim Maren

Important note
To cite this publication, please use the final published version (if applicable).
Please check the document version above.

Polystyrene nanoplastics are unlikely to aggregate in freshwater bodies[☆]

Februriyana Pirade [a,*], Jan Willem Foppen [a], Jan Peter van der Hoek [a,b], Kim Maren Lompe [a]

[a] Department of Water Management, Faculty of Civil Engineering and Geosciences, Delft University of Technology, Stevinweg 1, 2628 CN Delft, Netherlands
[b] Waternet, Korte Ouderkerkerdijk 7, 1096AC Amsterdam, Netherlands

ABSTRACT

The fate and toxicity of nanoplastics (NPs) in the environment is largely determined by their stability. We explored how water composition, nanoplastic size, and surface carboxyl group density influenced the aggregation of polystyrene (PS) NPs in fresh water. Unfunctionalized 200, 300, 500, and 1000 nm PS NPs and 310 nm carboxylated PS NPs with carboxyl group densities of 0.35 and 0.6 mmol g^{-1} were used to simulate pristine and aged NPs. Natural water matrices tested in this study include synthetic surface water (SSW), water from the Schie canal (Netherlands) and tap water. Suwannee River Natural Organic Matter (SRNOM) was included to mimic organic matter concentrations.

In $CaCl_2$, we found PS NPs are more stable as their size increases with the increase of the critical coagulation concentration (CCC) from 44 mM to 59 mM and 77 mM for NP sizes of 200 nm, 300 nm and 500 nm. Conversely, 1000 nm PS NPs remained stable even at 100 mM $CaCl_2$. Increasing the carboxyl group density decreased the stability of NPs as a result of the interaction between Ca^{2+} and the carboxyl group. These results were consistent with the mass of Ca^{2+} adsorbed per mass of NPs. The presence of SRNOM decreased the stability of PS NPs via particle bridging facilitated by SRNOM.

However, in SSW, Schie water and tap water with low divalent cation concentrations, the hydrodynamic size of PS NPs did not change, even at prolonged durations up to one week. We concluded that PS NPs are unlikely to aggregate in water with low divalent cation concentrations, like natural freshwater bodies. Ecotoxicologists and water treatment engineers will have to consider treating PS NPs as colloidally stable particles as the lack of aggregation in fresh surface water bodies will affect their ecotoxicity and may pose challenges to their removal in water treatment.

1. Introduction

Nanoplastics (NPs) are defined as plastic with dimensions between 100 nm and 1 μm (Gigault et al., 2021; Hartmann et al., 2019; Pradel et al., 2023). NPs have been detected quantified from various freshwater environments, including groundwater (Xu et al., 2022b), lakes (Materić et al., 2022), and rivers (Sullivan et al., 2020; Xu et al., 2022b). Their potential toxicity forms a threat to aquatic biota and human health (Sangkham et al., 2022; Xu et al., 2022a). They are also being detected in tap water (Li et al., 2022a; Xu et al., 2024a), which intensifies concerns about this emerging pollutant.

Research on behaviour of NPs, especially aggregation has gained significant interest (Li et al., 2021a; Oriekhova and Stoll, 2018; Parrella et al., 2024; Shiu et al., 2020; Yu et al., 2021). Understanding the aggregation and particle stability of NPs is crucial since they influence the fate, transport, ecotoxicity, and remediation of NPs. Stable, non-aggregated NPs are more bioavailable, increasing the risk of ingestion by aquatic organisms and facilitating more dispersion in surface water system (Bergami et al., 2017; Dong et al., 2019; Shen et al., 2019).

Past studies have examined NPs aggregation in controlled salt solutions, highlighting that higher salt concentration, cation valency (monovalent vs divalent cation), and interaction with natural organic matter (NOM) can change the aggregation of NPs. (Dong et al., 2021; Liu et al., 2020; Mao et al., 2020; Zhang et al., 2022). The co-presence of NOM and divalent cations can stabilize NPs or destabilize NPs. Stabilization occurs via electrostatic repulsion and/or steric repulsion when NOM is adsorbed to the surface of NPs via π-π interaction (Li et al., 2021a). Conversely, NPs can be destabilized via electrostatic attraction and/or by NOM via polymer bridging or by divalent ions via cation

---

bridging (Chhabra and Bassvaraj, 2019; Li et al., 2022b; Petosa et al., 2010)

Previous studies reported that the critical coagulation concentration (CCC) of NPs in a divalent ion system, such as CaCl$_2$, with and without NOM ranged between 13 mM and 32 mM (Table S1). The CCC represents the minimum concentration (mM) of an electrolyte needed to induce the destabilization of a colloidal suspension, with a higher CCC value indicating greater stability. However, in natural fresh surface water, the calcium (Ca^{2+}) concentrations are generally below 3 mM (Table S2) and the ionic strength (IS) is low to moderate, between 0.25 mM and 16.5 mM (Hammes et al., 2013). Previous studies on salts/electrolyte solutions have advanced our understanding of the NP's aggregation mechanism. However, the discrepancy between ion concentrations in a single salt solution and natural surface water could lead to different NP stability. Therefore, studying NP aggregation in realistic surface water matrices with typical ion and NOM compositions is essential for understanding their fate and ecological impact.

The physicochemical properties of NPs, in addition to the water matrix, are also pivotal factors influencing the stability of NPs. Environmental NPs (e-NPs) mainly originate from the weathering and fragmentation of larger plastics, due to photooxidation, introducing a wide range of particle sizes and oxygen-containing surface group (Alimi et al., 2022a; Xu et al., 2024b). Studies on nanoparticles and colloids suggest that smaller particles are inherently less stable compared to bigger particles in similar water matrix, due to higher Brownian motion and higher surface energy, leading to more frequent collisions and faster aggregation (Eastman, 2010; He et al., 2008). However, studies on the size effect on NPs aggregation have yielded mixed results, while some reported smaller NPs to be less (Liu et al., 2021), others found no size depndence (Alimi et al., 2022b).

Photooxidation also alters the chemical properties on the surface of NPs, introducing carboxyl groups which are prevalent in e-NPs (Blancho et al., 2021). Previous studies have attempted to simulate weathered e-NPs by exposing commercial NPs to accelerated aging using UV reactors or using carboxyl-modified NPS. Theoretically, we would expect that higher carboxyl groups density resulted in a more hydrophilic surface and more negative zeta potential, hence more stable particles (Liu et al., 2019). However, the aggregation of these simulated weathered NPs, specifically in CaCl2, showed varied outcomes. Some found that photooxidation promoted aggregation (Li et al., 2022b; Liu et al., 2019; Su et al., 2023; Xu et al., 2022c), while others observed increased stability (Yu et al., 2023). Similarly, studies using carboxylated PS NPs as model NPs for photo-oxidized PS reported both enhanced stability (Wu et al., 2023; Zhang et al., 2019) and increased aggregation (Wang et al., 2020; Zhu et al., 2022) compared to NPs without carboxyl group surface modifications in a CaCl$_2$ solution. Moreover (Yu et al., 2019), noted no difference in CCC between carboxyl-modified NPs and unfunctionalized NPs in CaCl$_2$ (Yu et al., 2019).

Size and carboxyl group density of NPs change the aggregation of NPs. However, the effect of these properties on NPs aggregation in typical surface water matrices with low ion concentrations is unexplored. The objective of our study was to understand the effect of particle size and increasing carboxyl group density on the aggregation of spherical PS NPs in freshwater conditions. We systematically examined the effect of particle size and carboxyl group density on the aggregation of NPs by employing four unfunctionalized PS NPs with different sizes (200, 300, 500, and 1000 nm) and two carboxyl-modified PS NPs with different carboxyl group densities (0.35 and 0.6 mmol g^{-1}). Various sizes of NPs represent the wide distribution of NPs in the aquatic environment, while different carboxyl group densities represent the degree of aging. Furthermore, we conducted comprehensive experiments using a well-defined water matrix that closely resembles surface water conditions (ion and NOM concentration), real surface water and tap water.

2. Material and methods

2.1. Preparation of nanoplastics and natural organic matter

This study used unfunctionalized polystyrene nanoplastic suspensions with particle diameters of 200 nm (NP$_{200}$), 300 nm (NP$_{300}$), 500 nm (NP$_{500}$), and 1000 nm (NP$_{1000}$) with 10% solids concentration purchased from Sigma-Aldrich, the Netherlands. Additionally, functionalized PS NPs of ~310 nm with carboxyl group densities of 0.35 mmol g^{-1} (NP-COOH$_{0.35}$) and 0.6 mmol g^{-1} (NP-COOH$_{0.6}$) were included to simulate environmental aging, characterized by the formation of oxygen-containing functional groups. All NP-COOH were synthesized following Pessoni et al. (2019) and provided by the Particle Engineering Centre, Department of Chemical Engineering NTNU Norway. Carboxyl group densities were quantified using the method of Li et al. (2019). The presence of COOH groups was confirmed by laser direct infrared (LDIR, Agilent) in hyperspectral mode from 975 to 1799 cm-1 with a step size of 4 cm^{-1}. Twenty discrete spectral measurements were conducted linearly and subsequently integrated to synthesize a composite spectrum. LDIR spectra showed a peak of C=O groups at 1720-1706 cm-1 (carboxylic acid) and 1750-1735 cm-1 (ester) (Fig. S1). Table S3 provided details on hydrodynamic size (D$_h$) and zeta potential (ζ) for all nanoplastics.

European surface water typically contains NOM, with concentrations ranging from 1 mg.L^{-1} to more than 10 mg.L^{-1} (Hammes et al., 2013). Suwanee River NOM (SRNOM 2R101N, IHSS) was selected as the model NOM for this investigation as an easily doseable full NOM isolate. SRNOM was prepared following methods in Pradel et al. (2021) and detailed in **Text S1**. The dissolved organic carbon (DOC) concentration of the stock SRNOM solution was determined using a TOC analyzer (Shimadzu). The DOC concentration of the stock solution was 225.91 ± 5.01 mg.DOC L^{-1}.

2.2. Preparation of water matrices

The aggregation kinetics of NPs were investigated in various aqueous media, including divalent salt solutions (CaCl$_2$, 1 mM–100 mM), synthetic surface water (SSW), filtered surface water from the Schie River (the Netherlands) and tap water (TW). CaCl$_2$ was selected due to the prevalence of divalent ions, especially calcium, in surface water, as reported by Arenas-Lago et al. (2019).

SSW, prepared following protocol by Smith et al. (2002), was used to provide NOM-free water with the same ion concentration as river water. It is to ensure that aggregation effects were solely attributable to the major ion chemistry of the water. The chemical composition was based on the Rhine water composition from the Lek canal as measured by the drinking water company Waternet, representing Dutch surface waters (2021). A comprehensive procedure for preparing the SSW can be found in **Text S2**.

Surface water from Schie River (predominantly Rhine water) was filtered through a 0.45 μm filter (Whatman Spartan 30/0.45 μm RC) to remove particles that could confound PS NP interactions and would be challenging to characterize. All solutions were stored at 4 °C until further use. The Ca^{2+} concentration for the SSW and filtered Schie Water (FSW) were 2.76 ± 0.020 mM, and 3.58 mM, respectively. Table S4 describes the major ion concentrations of SSW and filtered Schie water (FSW) measured by Ion Chromatography (Metrohm Compact IC Flex 930).

2.3. Aggregation experiments

Changes in D$_h$ were used to determine the aggregation of NPs (Singh et al., 2019; Wang et al., 2021). Measurements were perfomed using a Zetasizer Nano ZS (Malvern) at 25 °C with dynamic light scattering (DLS) at a 173° angle. Measurements were recorded every 10 s for 10 min. To investigate the effect of particle size, aggregation experiments were conducted based on particle number concentration to avoid

confounding effects. Stock solutions of NP_{200}, NP_{300}, NP_{500}, and NP_{1000}, were diluted to a working concentration of 2.27×10^{12} particles L^{-1} in $CaCl_2$ solutions (1–100 mM). This concentration equates to 10 mg.L^{-1} for NP_{200}, which was selected to improve data quality from the Zetasizer ZS measurement and commonly used in previous NPs aggregation studies. Details for calculating particle number concentration are provided in **Text S3** of the SI. All NPs were diluted directly inside the Zetasizer cuvette to a final volume of 1.5 mL and analyzed immediately.

To determine the relative effect of carboxyl groups, NOM, and the water matrix, only NP_{300} were used as the unfunctionalized NPs to match the nominal size of carboxylated NPs. Therefore, the effect of size, surface area, and particle number concentration can be excluded. For the carboxyl group density experiment, all NPs were prepared at 10 mg.L^{-1} in $CaCl_2$ solutions (1–100 mM) directly inside the Zetasizer cuvette. The effect of NOM was studied by repeating the previous procedure with the addition of 10 mg.DOC L^{-1}. In the experiment with NOM, the sequence was as follows: addition of SRNOM to the electrolyte solution followed by NPs ((Ca^{2+} + NOM) + NPs). This sequence simulated a condition where NPs are introduced as anthropogenic pollutants.

Finally, aggregation in natural surface water was tested using 10 mg.L^{-1} NP_{300}, NP-COOH$_{0.35}$, and NP-COOH$_{0.6}$ in SSW with and without the addition of 10 mg.DOC L^{-1}. The same sequence of solution additions was applied as in the experiment with $CaCl_2$, i.e. (water matrix + NOM) + NPs. The least stable NPs (lowest CCC in $CaCl_2$) were subsequently tested in FSW and TW. No additional NOM was added to natural water samples due to its inherent presence. The pH of all NPs was adjusted to 7.04 ± 0.033 prior to the mixing for all water matrices. All experiments were performed in triplicate unless stated otherwise.

2.4. Determination of the aggregation kinetics and attachment efficiencies

The aggregation rate (k, $seconds^{-1}$) was determined from the slope of the initial rate of change in hydrodynamic size (D_h, nm) as a function of time (t, seconds), according to (Chen and Elimelech, 2006):

$$k \propto \frac{1}{N_0} \left(\frac{dD_h(t)}{dt} \right)_{t \to 0} \tag{Eq 1}$$

with N_0 (particles.L^{-1} or mg.L^{-1}) represents the initial NPs concentration.

Aggregation rates k in the initial stage are typically associated with a reaction-limited aggregation (RLA) regime. This regime occurs under unfavourable conditions (i.e. low ionic strength) resulting in high electrostatic repulsion between particles. As the salt concentration increases, the electrostatic repulsion decreases, leading to a faster aggregation process. Ultimately, the particles become fully destabilized, reaching the maximum aggregation rate, k_{fast}, in favourable conditions or in the diffusion-limited aggregation (DLA) regime. The attachment efficiency (α, unitless) can be determined by normalizing aggregation rates obtained at a solution chemistry of interest to the rate constant for favourable conditions according to (Grolimund et al., 2001):

$$\alpha = \frac{k}{k_{fast}} = \frac{\frac{1}{N_0} \left(\frac{dD_h(t)}{dt} \right)_{t \to 0}}{\frac{1}{N_0} \left(\frac{dD_{h,fast}(t)}{dt} \right)_{t \to 0,}} \tag{Eq 2}$$

The subscript "fast" denotes favourable conditions. The experimental CCC value was determined from the intersection of extrapolated lines through the two regimes (Shams et al., 2020). A higher CCC value means greater stability for the particles.

2.5. Long-term stability of nanoplastics in synthetic and natural surface water

Long term stability of NPs in SSW was studied to determine the aggregation behavior of NPs in environmentally relevant water matrices.

Details on the procedure are provided in **Text S4.** In brief, 2.27×10^{12} particles L^{-1} of all unfunctionalized and carboxylated NPs were kept for 1 week in SSW_1 in an incubator shaker (Innova 44/44R) at 100 RPM, 25 °C with and without the addition of 10 mg.L^{-1} SRNOM. D_h and zeta potential (ζ-potential, in mV) of all NPs were measured periodically. Additionally, adsorption of NOM to NPs was determined as the reduction in NOM concentration. The least stable NPs were subsequently tested in FSW and TW. In all experiments, carbon-free borosilicate bottles were used to store NP suspensions throughout the experiment. The glassware cleaning procedure is provided in **Text S5.**

2.6. Calcium ion adsorption on NPs in a divalent ion system

A 24-h batch adsorption test was conducted to evaluate the adsorption of Ca^{2+} to PS NPs of different sizes and carboxyl group densities. Details on the procedure are provided in **Text S6.** In brief, NPs were kept in 2.5 mM $CaCl_2$ solutions for 24 h while being mixed in an incubator shaker (Innova 44/44R) at 100 RPM, 25 °C. After 24 h, all NPs samples were filtered with 0.2 μm PTFE filters to separate the unadsorbed Ca^{2+}. The filtration efficiency was verified by measuring NPs concentration in the filtrate via UV–Vis measurement. The Ca^{2+} concentration in the filtrate was analyzed using Ion Chromatography (Metrohm Compact IC Flex 930). Experiments were performed in duplicate.

3. Results

3.1. Aggregation of NPs in divalent ion solutions

3.1.1. Size-dependent aggregation of PS NPs

The aggregation of PS NPs in divalent solutions showed two distinct aggregation profiles (Fig. S2). The hydrodynamic size of NP_{200}, NP_{300}, and NP_{500} in $CaCl_2$ solution increased as a function of time and increasing ion concentration (Figure S2 a, b, and c). NP_{200}, NP_{300}, and NP_{500} started to aggregate at CaC_2 concentration higher than 10 mM, 30 mM, and 60 mM, respectively. The aggregation was constant above 40 mM, 50 mM, and 70 mM for NP_{200}, NP_{300}, and NP_{500}, respectively, suggesting the complete elimination of energy barriers. Accordingly, the ζ values showed that the stability of NPs reduced as the $CaCl_2$ concentration increased (Table S5). In contrast, NP_{1000} exhibited exceptional stability within the tested $CaCl_2$ concentration range (Figure S2 d).

Fig. 1 depicts the α for each $CaCl_2$ concentration for all tested NPs. The CCC of PS NPs in $CaCl_2$ solution increased as the size increased, with
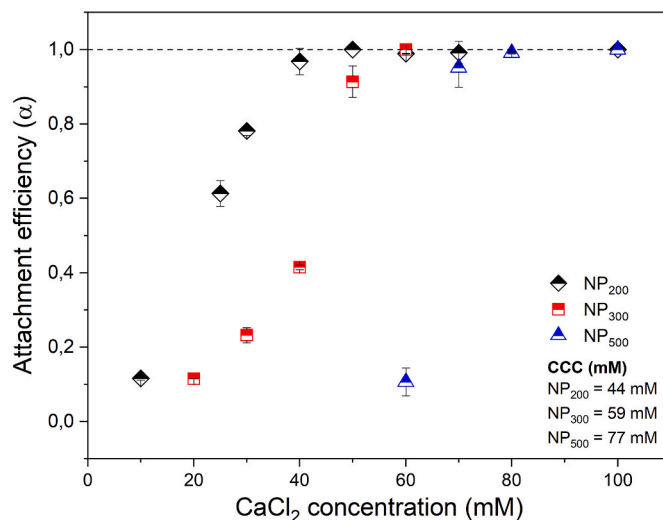

Fig. 1. Attachment efficiency and calculated CCC value of 2.27×10^{12} particle L^{-1} of NP_{200}, NP_{300}, NP_{500} in $CaCl_2$. Error bars represent the standard deviation of three replicates.

CCC of 44 mM for NP_{200}, 59 mM for NP_{300}, and 77 mM for NP_{500}, indicating larger NPs particles were more stable. The attachment efficiencies of NP_{1000} were not calculated because they remained stable in all tested $CaCl_2$ concentrations; hence, we proposed the CCC of NP_{1000} is higher than 100 mM. According to the CCC values, the tendency of PS NPs to aggregate in divalent ion solutions followed the order of $NP_{200} > NP_{300} > NP_{500} > NP_{1000}$, where aggregation occurs at lower salt concentrations for smaller particles.

The batch adsorption test (Table S6) showed that bigger NPs adsorb less Ca^{2+} per mass of NPs. The amount of Ca^{2+} adsorbed onto NP_{200}, NP_{300}, NP_{500}, and NP_{1000} was 1.030 ± 0.51 mg mg NPs^{-1}, 1.018 ± 0.11 mg mg NPs^{-1}, 0.137 ± 0.01 mg mg NPs^{-1}, and 0.021 ± 0.0 mg mg NPs^{-1}; respectively.

3.1.2. Carboxyl group density increased aggregation of similar size PS NPs

The attachment efficiency of unfunctionalized NP_{300} and functionalized NP-COOH is depicted in Fig. 2. Both NP-COOH have lower CCC values than unfunctionalized NP_{300}, indicating they were less stable. Furthermore, higher carboxyl group density resulted in higher aggregation potential. However, doubling the carboxyl group density from 0.35 mmol g^{-1} to 0.6 mmol g^{-1} did not result in a proportional decrease in CCC values. CCC of NP_{300}, NP PS-$COOH_{0.35}$ and PS-$COOH_{0.6}$ were 86, 75 and 62 mM, respectively. Based on the CCC values, the aggregation of unfunctionalized-functionalized NPs follows the order of NP-$COOH_{0.6} >$ NP-$COOH_{0.35} > NP_{300}$.

A comparison between NP-COOH and NP_{200} yielded contradictory results. Figs. 1 and 2 show that NP-COOH yielded a higher CCC value than unfunctionalized NP_{200} under the same mass concentration of 10 mg/L. CCC of NP_{200}, NP-$COOH_{0.35}$, and NP-$COOH_{0.6}$ were 44 mM, 75 mM, and 62 mM, respectively. These CCCs indicated that the carboxyl group on the surface of NPs increased the stability of NPs. However, we attributed these outcomes to the higher particle number concentration of NP_{200}, which leads to more particle collision frequencies. When the experiment was repeated under the same particle number concentration of 2.27×10^{12} particles.L^{-1}, NP-$COOH_{0.6}$ aggregated rapidly at ~40 mM, which was lower than the CCC of NP_{200} (Fig. S3). This result suggested that NP-$COOH_{0.6}$ were less stable than NP_{200}, consistent with the comparison between NP_{300} and NP-COOH. Accordingly, NP-COOH also adsorbed more Ca^{2+}, where NP-$COOH_{0.6}$ and NP-$COOH_{0.35}$ adsorbed 1.031 ± 0.02 mg.mgNPs^{-1} and 1.203 ± 0.20 mg.mgNPs^{-1}, respectively. Overall, our observations showed that addition of carboxyl group on the surface of NPs increased the aggregation of PS NPs.
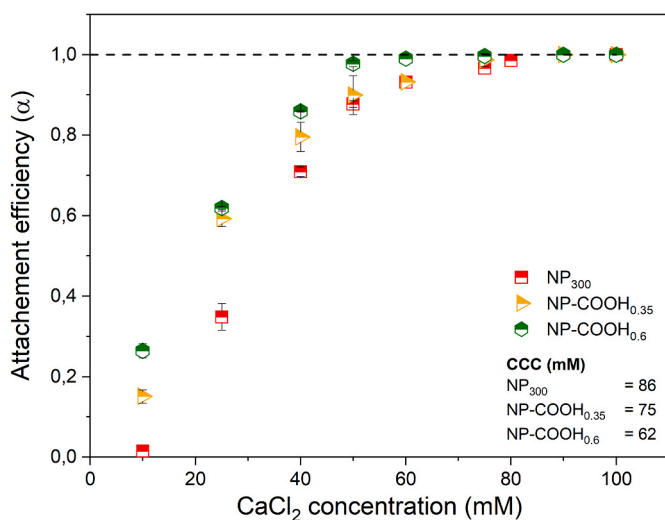
3.1.3. Effect of NOM

SRNOM was used to determine the effect of NOM on the aggregation of NPs in a divalent ion system. Fig. 3 illustrates the CCC of NP_{300}, NP-$COOH_{0.35}$, and NP-$COOH_{0.6}$ in $CaCl_2$ with and without the addition of SRNOM. In the presence of 10 mg.L^{-1} SRNOM, all NPs were more prone to aggregation, as indicated by lower CCC value compared to no addition of SRNOM. CCC values of NP_{300}, NP-$COOH_{0.35}$, and NP-$COOH_{0.6}$ reduced to 50 mM, 34 mM, and 33 mM, respectively. Unfunctionalized NP_{300} had the highest stability in $CaCl_2$ + NOM solution, indicated that NOM destabilized carboxylated NPs more effectively than unfunctionalized NPs. Interestingly, although the CCC of NP-$COOH_{0.6}$ was lower than NP-$COOH_{0.35}$ in the absence of NOM, they have similar CCC values with the addition of SRNOM. The changes in ζ-potential values of NP-$COOH_{0.35}$ and NP-$COOH_{0.6}$ were also comparable (Table S7). This observation indicated that NPs were destabilized by other forces in addition to the electrostatic interaction.

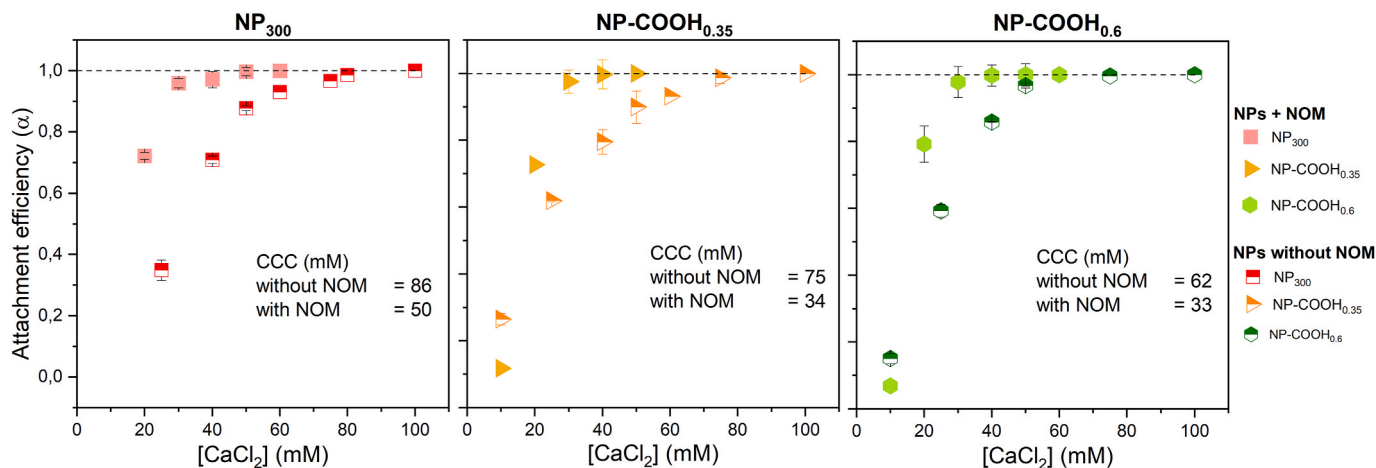### 3.2. Aggregation of PS NPs in synthetic surface water and natural water

No aggregation of 10 mg.L^{-1} PS NP_{300}, NP-$COOH_{0.35}$, and NP-$COOH_{0.6}$ was observed in synthetic surface water with low Ca^{2+} and other major ion concentrations in short (Fig. S4a) and over a week of observation (Fig. 4a). These results were in agreement with the aggregation experiment in $CaCl_2$, in which NPs did not aggregate in low Ca^{2+} concentration. The Ca^{2+} ion concentration in SSW, at 2.76 mM, was insufficient to screen NPs charges as suggested by the ζ-potential value (Table S8).

Furthermore, adding 10 mgDOC.L^{-1} NOM did not destabilized NP_{300}, NP-$COOH_{0.35}$, and NP-$COOH_{0.6}$ over the short aggregation experiment (Fig. S4b). The long-term stability experiment also showed that they remained stable in SSW + NOM (Fig. 4b) even after 5 days, with ζ-potential values indicating good particle stability (Table S9). Additionally, the measurement of UV_{280} showed that the NOM concentration was reduced by only 1.2%, 2.43%, and 4.76% for NP_{300}, NP-$COOH_{0.35}$, and NP-$COOH_{0.6}$, respectively. In FSW and TW, NP-$COOH_{0.6}$ which had the lowest stability in $CaCl_2$ solutions, also remained stable (Fig. S4c). The DOC concentrations of these water matrices were 1.76 ± 0.036 mg.DOC L^{-1} for TW and 17.94 ± 0.22 mg.DOC L^{-1} for FSW. The DOC concentration of FSW was higher than our tested SRNOM concentration. This result indicated that the destabilization effect of SRNOM was not present in water with low Ca^{2+} concentration, regardless of the NOM concentration. The prolonged experiment of NP-$COOH_{0.6}$ in FSW and TW also showed that NPs remained stable, although the size of NP-$COOH_{0.6}$ increased by 16–18% (Fig. 4c). Measurement of D_h in FSW without NPs addition shows there were existing particles and/or colloids that continue to aggregate and become larger than 700 nm and could possibly affect the measurement (Fig. S4d).

4. Discussion

4.1. Physicochemical properties of NPs change their aggregation in a divalent ion system

Aggregations of NPs were studied in divalent ion solutions, $CaCl_2$, to determine the effect of size, carboxyl group, and NOM addition. Table S10 summarizes the comparison of CCC values from all NPs in our study concerning their initial concentration (particle number concentration or mass concentration). In divalent ion solution without the addition of SRNOM, aggregation of NPs at high Ca^{2+} concentration was caused by the compression of the electrical double layer surrounding NPs, which weakened the repulsive forces between NPs. Consequently, van der Waals attraction dominated and led to aggregation (Petosa et al., 2010). Our observations showed that the aggregation of NPs in divalent ion systems was size-dependent, meaning higher $CaCl_2$ concentrations were required to fully destabilized bigger NPs. The changes in ζ-values over the concentration of $CaCl_2$ confirmed that Ca^{2+} could screen the

Fig. 2. Attachment efficiency of 10 mg.L^{-1} NP_{300}, NP-$COOH_{0.35}$, and NP-$COOH_{0.6}$ in $CaCl_2$. Error bars represent the standard deviation of three replicates.

Fig. 3. Attachment efficiencies of (a) NP$_{300}$, (b) NP-COOH$_{0.35}$, (c) NP-COOH$_{0.6}$ with and without the addition of 10 mg.DOC L^{-1} SRNOM. Error bars represent standard deviation (n = 3).
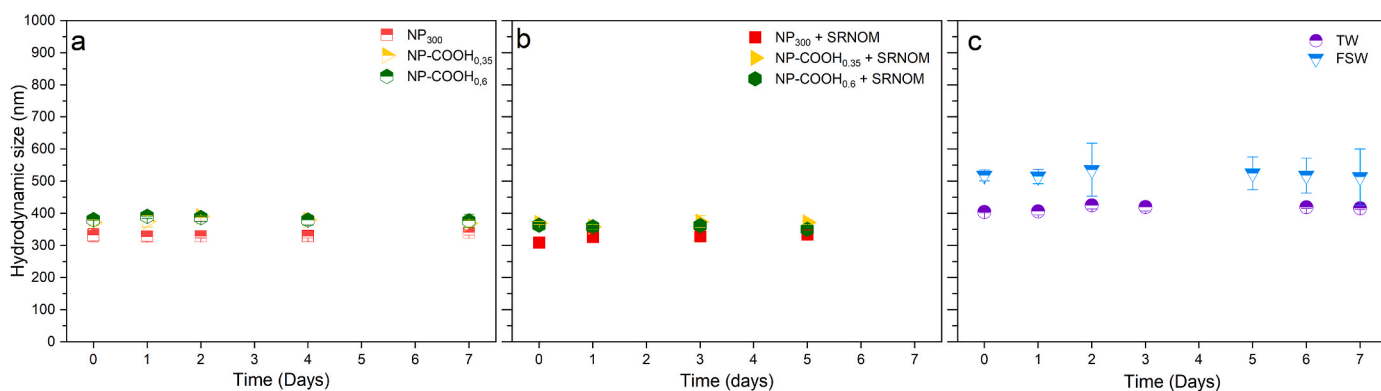
Fig. 4. (a) D$_h$ of NP$_{300}$, NP-COOH$_{0.35}$, and NP-COOH$_{0.6}$ over a week observation in SSW without and (b) with 10 mgDOC.L^{-1} SRNOM. (c) D$_h$ of NP-COOH$_{0.6}$ in TW and FSW over a week of observation. Error bars represent the standard deviation of three samples.

surface charge of NPs, and the effect was more pronounced in smaller particles (Table S5). Furthermore, the Ca^{2+} adsorption experiment (Table S6) showed that smaller NPs particles adsorb more Ca^{2+} per mass of plastic. Smaller particles are generally more reactive owing to their higher surface area-to-volume ratio (He et al., 2008). Adsorption is a surface phenomenon, and a higher surface area-to-volume ratio provides more active sites for cation to adsorb to the surface. Therefore, the higher adsorption of Ca^{2+} in smaller particles is likely to be one of the reasons why smaller NPs in this study aggregated at lower salt concentrations. Similarly, Zhang et al. (2022) observed stronger adsorption capacity of lead ion (Pb^{2+}) by 30 nm PS NPs compared to 100 nm PS NPs, leading to higher aggregation potential in smaller NPs.

Our observation also showed the effect of Brownian motion on the aggregation tendency of NPs. Previous studies attributed the greater stability of larger NPs particles to a lower particle number concentration and, consequently, lower particle collision frequencies (Alimi et al., 2022b; Li et al., 2021b; Sun et al., 2021a). Considering the particle number concentration in all tested NPs was the same, the better stability in larger NPs sizes is more likely due to a lower Brownian motion in larger particles. In the case of NP$_{1000}$, the ζ-value at concentrations of 100 mM CaCl$_2$ (Table S5) indicated that aggregation should be observed due to charge screening by Ca^{2+}. However, no aggregation was observed, indicating other forces/interactions stabilized the particles. Sun et al. (2021b) reported that the buoyant force controlled the aggregation of 1000 nm PS NPs. Therefore, a fluid shear is required to induce aggregation of 1000 nm NPs.

In a divalent ion system, NPs were destabilized by the compression of

EDL and electrostatic interactions. Smaller NPs were more prone to aggregation because 1) their higher surface-to-volume ratio, which increases Ca^{2+} adsorption, and 2) greater Brownian motion, which enhances particle collisions. Size-dependent aggregation of PS NPs in divalent ion solutions was also reported in other studies (Li et al., 2021b; Liu et al., 2021; Zhang et al., 2022). Although earlier studies using mass concentration found smaller NPs had higher aggregation potential, these results were influenced by collision frequencies. The effect of particle collision will be more pronounced in larger particles (i.e. 500 nm). For instance, at 10 mg/L, NP$_{500}$ remained stable at a high CaCl$_2$ concentration of up to 100 mM (Fig. S5), aligning with findings by Liu et al. (2021). Similarly, NP$_{300}$ destabilized at higher CaCl$_2$ concentrations in mass-based measurements compared to particle number, with CCCs of 86 mM and 59 mM, respectively.

Regarding surface functionality, the carboxylated group on the surface of NPs increased the destabilization, following the order of NP-COOH$_{0.6}$ > NP-COOH$_{0.35}$ > NP$_{300}$. Changes in ζ-potential values indicated that Ca^{2+} screened the charge of NP-COOH more effectively, despite their more negative charge in MilliQ-water compared to unfunctionalized NPs (Table S3 and Table S5). The effect is most pronounced in NP-COOH$_{0.6}$ which has the highest carboxyl group density. Previous research has indicated a strong binding between carboxyl group and Ca^{2+}, which increased the affinity of NPs for binding with Ca^{2+} ions (Bala et al., 2007). Our result confirmed that NP-COOH$_{0.6}$ exhibited the highest Ca^{2+} adsorption (Table S6). Similar Ca^{2+} adsorption has been observed for carboxylated nanoparticles such as fullerene (Qu et al., 2010) and colloids such as biochar (Wang et al., 2019). Our

findings also align with previous studies showing increased aggregation in aged NPs due to the formation of additional carboxyl groups (Li et al., 2022b; Liu et al., 2019; Xu et al., 2022c).

Particle size did not outweigh the effect of COOH-Ca^{2+} interaction when NPs had similar sizes (NP$_{300}$ vs NP-COOH) or similar particle number concentrations (Table S10, CCC NP$_{200}$ vs NP-COOH particle number concentration-based). However, the effect of the carboxyl group on aggregation was confounded by the collision frequency when measured based on the mass concentration (Table S10, CCC NP$_{200}$ vs NP-COOH mass concentration-based). The interplay between increasing carboxyl group density and decreasing NP size, which increases particle concentration, hasn't been explicitly addressed in previous aggregation studies and should be examined. The effect of physicochemical properties on NP aggregation can be better assessed when experiments are conducted at equal particle numbers. The reason is that collision frequencies are largely influenced by the particle number in the solution. Considering that the aging experiment can both decrease the particle size and increase the carboxyl density of nanoplastic, lab studies investigating the effect of aging on NPs should measure the particle number concentration.

4.2. NOM decreased the stability of NPs in a divalent ion system

Table S10 shows that adding 10 mg.L^{-1} NOM decreased the CCC and increased the aggregation of unfunctionalized (NP$_{300}$) and carboxylated NPs (NP-COOH$_{0.35}$ and NP-COOH$_{0.6}$). SRNOM is mainly comprised of humic acid with abundant oxygen-containing functional groups, including carboxyl groups on its surface (Driver and Perdue, 2014; Fu et al., 2019). These functional groups give SRNOM a negative charge, similar to NPs. For this reason, adding a high SRNOM concentration should improve the stability of NPs due to electrostatic repulsion and/or steric hindrance. When mixed with SRNOM alone without Ca^{2+} cation, the ζ-potential value of NPs became more negative and no aggregation was observed over 24 h, indicating NPs were stabilized by electrostatic repulsion (Fig. S6). However, in the presence of NOM and Ca^{2+}, the ζ-potential value changed, and NPs were destabilized as the cation concentration increased (Table S7). Since ζ-potential values between NPs and NPs + NOM across all CaCl$_2$ concentrations were similar, the increased aggregation of NP + NOM was unlikely attributed to electrostatic interaction alone but also to molecular bridging between NPs and SRNOM facilitated by Ca^{2+}.

It has been proposed that NOM can adsorb onto the surface of NPs through hydrophobic and π-π interactions, thereby covering the surface and increasing the stability of NPs (Liu et al., 2020; Xu et al., 2022c). Yu et al. (2019) suggested that the stabilization effect of SRNOM is concentration-dependent. At a low concentration (<5 mg.L^{-1}), SRNOM increased the stability of NPs. However, at a high concentration SRNOM promoted the destabilization of NPs because unadsorbed SRNOM binds with Ca^{2+}. Eventually, the SRNOM aggregates destabilized NPs through polymer bridging. The proposed mechanism is likely to occur in a system where SRNOM can effectively adsorb to NPs and electrostatic interactions between negatively charged NOM or NPs and Ca^{2+} cations are minimal. For instance, this could happen in experiments where a NPs + NOM mixture is added to a divalent cation solution (Kong et al., 2023) or in a solution with a low divalent cation concentration. However, our system introduced NPs to a mixture containing Ca^{2+} cations and NOM to simulate a condition where NPs enter the aquatic environment as a pollutant. We argue that in such a system, the initial interaction between Ca^{2+} and NOM will first destabilize NOM through electrostatic attraction. Then, when NPs are introduced, NOM aggregates bridge the NPs through polymer bridging and cause destabilization of NPs. We conducted additional experiments to investigate the destabilization mechanism of NPs at a low SRNOM concentration. Repeating the NOM aggregation procedure for NP-COOH$_{0.6}$ with 2 mg.L^{-1} SRNOM showed that NP-COOH$_{0.6}$ aggregated and the calculated CCC is 51 mM (Fig. S7). This result indicated that the co-presence of NOM and Ca^{2+} cations can

destabilize NPs in both low and high NOM concentrations through polymer bridging. The destabilization effect is more pronounced as the NOM concentration increases. Similar destabilization mechanisms were observed for other nanoparticles such as C$_{60}$ fullerenes (Chen and Elimelech, 2006) and zero-valent iron (Dong and Lo, 2013). Destabilization of NPs in the presence of Ca^{2+} and low concentrations of various NOM types was also observed in another study (Liu et al., 2020). Further, we found that for NP-COOH, doubling the carboxyl group density from 0.35 mmol g^{-1} to 0.6 mmol g^{-1} did not change the CCC greatly. This result is similar to that of a previous study by Xu et al. (2022c).

4.3. Nanoplastics remained stable in synthetic surface water and natural surface water

It is important to note that NPs only aggregated in high concentrations of divalent ions (Table S10), regardless of their size and carboxyl group density or the absence or presence of high or low NOM concentration. In SSW with a Ca^{2+} concentration of 2.7 mM, no aggregation of NPs over the short or prolonged experiments was observed. The low concentration of Ca^{2+} in SSW was not sufficient to electrostatically destabilize NPs via electrostatic interactions as reflected by the ζ-potential values (Table S8). In the presence of NOM, NPs were also generally stable. We attributed the stability of NPs in SSW + NOM to electrostatic interaction (repulsion) rather than steric stabilization due to NOM adsorption. The D$_h$ of NPs was relatively stable with an increase in size of less than 8%. Furthermore, the reduction of NOM concentration after 5 days was insignificant, indicating NOM was not effectively adsorbed. Similar to the observation in SSW, NPs remained stable in FSW and TW over 10 min of the aggregation experiment and remained stable after a week. NPs in FSW had a 16–18% size increase compared to the NPs control in MQ water (data not shown). Since FSW was filtered through 0.45 μm, natural colloids or microorganisms that are smaller than 0.45 μm and naturally existed in FSW (Fig. S4d) might be adsorbed to the surface of NP-COOH$_{0.6}$. However, the adsorbed material did not cause aggregation, as the size of NP-COOH$_{0.6}$ remained stable over 7 days of observation and the increases in size were less than 1.5x. It is possible that the adsorbed material provided steric stabilization for NPs upon their adsorption. The absence of electrolytes also did not result in aggregation in a solution containing NPs, extracellular polymeric substances (EPS) and fulvic acid-rich NOM in previous studies (Xiong et al., 2023; Zhang et al., 2019). Zhang et al. (2019) also reported that carboxyl-modified NPs were stable in low divalent ion concentrations during long-term observation of 21 days NPs.

Our result and those from previous studies suggest that aggregation of NPs in surface water was influenced by the cation concentration rather than natural organic matter concentration. At lower divalent ion concentrations, the electrostatic repulsion stabilized negatively charged NPs as the available cation could not screen NPs charge and compress the EDL. Therefore, no aggregation is observed regardless of the NOM concentration.

Furthermore, we would like to mention that Blancho et al. (2021) estimated that the surface of e-NPs contained 32 ± 6% of oxidized functional groups with ~10% being carboxylic groups, and equal to 0.225 ± 8.5e^{-3} mmol g^{-1} were proton-reactive sites. The number of the proton-reactive sites was slightly less than the carboxyl group of NPs tested in this study, which were only aggregated in high Ca^{2+} concentration. This comparison implied that e-NPs might also only aggregate in the presence of high divalent cation concentrations, which is atypical for surface water.

4.4. Implications and outlook

Aggregation alters the size distribution of NPs and decreases the surface area of NPs, which might, in turn, impact their adsorption capacity for toxins, their mobility and bioavailability. On the one hand, small and stable NPs can increase bioavailability and ecotoxicity. For

instance, Zhang et al. (2019) observed a 100% immobilisation rate of *D. magna* by stable NPs. On the other hand, Wu et al. (2019) reported that that aggregated NPs formed flocs that entangled *D. magna*, reducing its survival rate. Considering the high stability of NPs observed in our study, we suggest including non-aggregated NPs in relevant water matrices with low ionic concentrations in ecotoxicity studies.

Stable NPs remain dispersed in water and mobile, potentially increasing their travel distance (Dong et al., 2019). Consequently, NPs can spread to distant locations and potentially reach water treatment installations. Fresh surface water systems like lakes and rivers, are commonly used as sources for drinking water treatment plants. Surface water treatment plants in the Netherlands reported low concentrations of divalent ions in their intake water, not exceeding 1.8 mM for Ca^{2+} (internal survey, data not shown). Understanding the stability of NPs in fresh surface water can help design better remediation strategies to increase the NPs removal efficiency in WTP. For instance, targeting the removal of stable NPs simultaneously with colloids of similar sizes via coagulation/flocculation unit (Sun et al., 2019).

This study examined the impact of NP size and carboxyl group density on aggregation, but other physicochemical properties should also be considered. Studies that reported NP CCC values in $CaCl_2 < 10$ mM (Fig. S8) indicate that NPs shape greatly influences aggregation behavior. Pradel et al. (2021) noted that the irregularly shaped NPs tend to form bigger aggregates in monovalent ion solutions compared to spherical NPs. Dong et al. (2021) also highlighted that non-uniform shapes and sizes of NPs as a property that could lead to aggregation within the range of typical Ca^{2+} concentration in freshwater used in water treatment plants.

5. Conclusions

Nanoplastics have been detected in various aquatic environments. The study presented here revealed the importance of the physicochemical properties of NPs and water chemistry, especially cation (Ca^{2+}) and NOM, on the destabilisation of NPs. Under high divalent ion concentrations, physicochemical properties (i.e size and surface functional group) changed the aggregation of NPs. In this type of water and under the same particle number concentration, aggregation of PS NPs was size-dependent. Furthermore, the interaction between COOH groups and Ca^{2+} increased the aggregation potential. Both low and high NOM concentrations further destabilized NPs via polymer bridging with NOM aggregates. Our results indicate that small NPs with oxygencontaining surface groups can easily aggregate in waters with high cation concentrations, such as seawater or estuaries.

In contrast, NPs are unlikely to aggregate in fresh surface water because their aggregation occurs primarily due to electrostatic interaction. In this type of water, low concentrations of Ca^{2+} could not screen NPs charge, leading to stabilization through electrostatic repulsion. Similarly, adding NOM does not promote particle bridging due to the low Ca^{2+} concentration. Our study indicated that the destabilization of PS NPs required a high Ca^{2+} cation concentration (>33 mM). Therefore, polystyrene NPs, regardless of the size and carboxyl-group density, are most likely to remain stable in fresh surface water environments where Ca^{2+} concentration is typically lower than 3 mM.

Lastly, particle number concentration, often overlooked when comparing NPs with different physical properties, affects NPs aggregation. Higher concentrations increase collision frequency, enhancing aggregation potential, particularly in larger NPs (500 nm in this study). The concentration used in our study is higher than the expected e-NPs concentration in surface water, which is around 10^7 particles.L^{-1} (Xu et al., 2022b). For this reason, in surface water the collision between NPs is likely to be minimal. Recently Lins et al. (2022) modelled the aggregation of NPs in relevant environmental concentrations (10^{-2} μg.L^{-1}), which is experimentally challenging due to analytical limitations. Their study suggested that in low salinity waters (10 mM NaCl), NPs between 100 and 1000 are likely to remain as single particles even with high

colloid levels up to 40 mg.L^{-1}. Thus, future studies on the effect of NPs, such as ecotoxicity or remediation of NPs, should consider PS NPs as colloidally stable particles under typical fresh surface water conditions.

Declaration of competing interest

The authors declare that they have no known competing financial interests or personal relationships that could have appeared to influence the work reported in this paper.

Appendix A. Supplementary data

Supplementary data to this article can be found online at https://doi.org/10.1016/j.envpol.2024.125393.

Data availability

Data will be made available on request.

References

Alimi, O.S., Claveau-Mallet, D., Kurusu, R.S., Lapointe, M., Bayen, S., Tufenkji, N., 2022a. Weathering pathways and protocols for environmentally relevant microplastics and nanoplastics: what are we missing? J. Hazard Mater. 423, 126955. https://doi.org/10.1016/j.jhazmat.2021.126955.

Alimi, O.S., Farner, J.M., Rowenczyk, L., Petosa, A.R., Claveau-Mallet, D., Hernandez, L. M., Wilkinson, K.J., Tufenkji, N., 2022b. Mechanistic understanding of the aggregation kinetics of nanoplastics in marine environments: comparing synthetic and natural water matrices. J. Hazard. Mater. Adv. 7, 100115. https://doi.org/10.1016/j.hazadv.2022.100115.

Arenas-Lago, D., Abdolahpur Monikh, F., Vijver, M.G., Peijnenburg, W.J.G.M., 2019. Dissolution and aggregation kinetics of zero valent copper nanoparticles in (simulated) natural surface waters: simultaneous effects of pH, NOM and ionic strength. Chemosphere 226, 841–850. https://doi.org/10.1016/j.chemosphere.2019.03.190.

Bala, T., Prasad, B.L.V., Sastry, M., Kahaly, M.U., Waghmare, U.V., 2007. Interaction of different metal ions with carboxylic acid group: a quantitative study. J. Phys. Chem. A 111, 6183–6190. https://doi.org/10.1021/jp067906x.

Bergami, E., Pugnalini, S., Vannuccini, M.L., Manfra, L., Faleri, C., Savorelli, F., Dawson, K.A., Corsi, I., 2017. Long-term toxicity of surface-charged polystyrene nanoplastics to marine planktonic species Dunaliella tertiolecta and Artemia franciscana. Aquat. Toxicol. 189, 159–169. https://doi.org/10.1016/j.aquatox.2017.06.008.

Blancho, F., Davranche, M., Fumagalli, F., Ceccone, G., Gigault, J., 2021. A reliable procedure to obtain environmentally relevant nanoplastic proxies. Environ. Sci.: Nano 8, 3211–3219. https://doi.org/10.1039/d1en00395j.

Chen, K.L., Elimelech, M., 2006. Aggregation and deposition kinetics of fullerene (C60) nanoparticles. Langmuir 22, 10994–11001. https://doi.org/10.1021/la062072v.

Chhabra, R., Bassvaraj, M.G., 2019. Colloidal dispersions. In: Coulson and Richardsons's Chemical Engineering. Butterworth-Heinemann, pp. 693–737. https://doi.org/10.1038/171142a0.

Dong, H., Lo, I.M.C., 2013. Influence of calcium ions on the colloidal stability of surface-modified nano zero-valent iron in the absence or presence of humic acid. Water Res. 47, 2489–2496. https://doi.org/10.1016/j.watres.2013.02.022.

Dong, S., Cai, W., Xia, J., Sheng, L., Wang, W., Liu, H., 2021. Aggregation kinetics of fragmental PET nanoplastics in aqueous environment: complex roles of electrolytes, pH and humic acid. Environ. Pollut. 268, 115828. https://doi.org/10.1016/j.envpol.2020.115828.

Dong, Z., Zhu, L., Zhang, W., Huang, R., Lv, X.W., Jing, X., Yang, Z., Wang, J., Qiu, Y., 2019. Role of surface functionalities of nanoplastics on their transport in seawater-saturated sea sand. Environ. Pollut. 255, 113177. https://doi.org/10.1016/j.envpol.2019.113177.

Driver, S.J., Perdue, E.M., 2014. Acidic functional groups of suwannee river natural organic matter, humic acids, and fulvic acids. ACS Symp. Ser. 1160, 75–86. https://doi.org/10.1021/bk-2014-1160.ch004.

Eastman, J., 2010. Stability of charge-stabilised colloids. In: Cosgrove, T. (Ed.), Colloid Science: Principles, Methods and Applications. John Wiley & Sons, Inc., pp. 45–59

Fu, H., Liu, K., Alvarez, P.J.J., Yin, D., Qu, X., Zhu, D., 2019. Quantifying hydrophobicity of natural organic matter using partition coefficients in aqueous two-phase systems. Chemosphere 218, 922–929. https://doi.org/10.1016/j.chemosphere.2018.11.183.

Gigault, J., El Hadri, H., Nguyen, B., Grassl, B., Rowenczyk, L., Tufenkji, N., Feng, S., Wiesner, M., 2021. Nanoplastics are neither microplastics nor engineered nanoparticles. Nat. Nanotechnol. https://doi.org/10.1038/s41565-021-00886-4.

Grolimund, D., Elimelech, M., Borkovec, M., 2001. Aggregation and deposition kinetics of mobile colloidal particles in natural porous media. Colloids Surfaces A Physicochem. Eng. Asp. 191, 179–188. https://doi.org/10.1016/S0927-7757(01)00773-7.

Hammes, J., Gallego-Urrea, J.A., Hassellöv, M., 2013. Geographically distributed classification of surface water chemical parameters influencing fate and behavior of nanoparticles and colloid facilitated contaminant transport. Water Res. 47, 5350–5361. https://doi.org/10.1016/j.watres.2013.06.015.

Hartmann, N.B., Hüffer, T., Thompson, R.C., Hassellöv, M., Verschoor, A., Daugaard, A. E., Rist, S., Karlsson, T., Brennholt, N., Cole, M., Herrling, M.P., Hess, M.C., Ivleva, N. P., Lusher, A.L., Wagner, M., 2019. Are we speaking the same language? Recommendations for a definition and categorization framework for plastic debris. Environ. Sci. Technol. 53, 1039–1047. https://doi.org/10.1021/acs.est.8b05297.

He, Y.T., Wan, J., Tokunaga, T., 2008. Kinetic stability of hematite nanoparticles: the effect of particle sizes. J. Nanoparticle Res. 10, 321–332. https://doi.org/10.1007/s11051-007-9255-1.

Kong, Y., Li, X., Tao, M., Cao, X., Wang, Z., Xing, B., 2023. Cation-π mechanism promotes the adsorption of humic acid on polystyrene nanoplastics to differently affect their aggregation: evidence from experimental characterization and DFT calculation. J. Hazard Mater. 459, 132071. https://doi.org/10.1016/j.jhazmat.2023.132071.

Li, M., Cheng, F., Xue, C., Wang, H., Chen, C., Du, Q., Ge, D., Sun, B., 2019. Surface modification of stöber silica nanoparticles with controlled moiety densities determines their cytotoxicity profiles in macrophages. Langmuir 35, 14688–14695. https://doi.org/10.1021/acs.langmuir.9b02578.

Li, X., He, E., Jiang, K., Peijnenburg, W.J.G.M., Qiu, H., 2021a. The crucial role of a protein corona in determining the aggregation kinetics and colloidal stability of polystyrene nanoplastics. Water Res. 190, 116742. https://doi.org/10.1016/j.watres.2020.116742.

Li, X., He, E., Xia, B., Liu, Y., Zhang, P., Cao, X., Zhao, L., Xu, X., Qiu, H., 2021b. Protein corona-induced aggregation of differently sized nanoplastics: impacts of protein type and concentration. Environ. Sci.: Nano 8, 1560–1570. https://doi.org/10.1039/d1en00115a.

Li, X., Ji, S., He, E., Peijnenburg, W.J.G.M., Cao, X., Zhao, L., Xu, X., Zhang, P., Qiu, H., 2022b. UV/ozone induced physicochemical transformations of polystyrene nanoparticles and their aggregation tendency and kinetics with natural organic matter in aqueous systems. J. Hazard Mater. 433, 128790. https://doi.org/10.1016/j.jhazmat.2022.128790.

Li, Y., Wang, Z., Guan, B., 2022a. Separation and identification of nanoplastics in tap water. Environ. Res. 204. https://doi.org/10.1016/j.envres.2021.112134.

Lins, T.F., O'Brien, A.M., Zargartalebi, M., Sinton, D., 2022. Nanoplastic state and fate in aquatic environments: multiscale modeling. Environ. Sci. Technol. 56, 4017–4028. https://doi.org/10.1021/acs.est.1c03922.

Liu, L., Song, J., Zhang, M., Jiang, W., 2021. Aggregation and deposition kinetics of polystyrene microplastics and nanoplastics in aquatic environment. Bull. Environ. Contam. Toxicol. 107, 741–747. https://doi.org/10.1007/s00128-021-03239-y.

Liu, Y., Hu, Y., Yang, C., Chen, C., Huang, W., Dang, Z., 2019. Aggregation kinetics of UV irradiated nanoplastics in aquatic environments. Water Res. 163, 114870. https://doi.org/10.1016/j.watres.2019.114870.

Liu, Y., Huang, Z., Zhou, J., Tang, J., Yang, C., Chen, C., Huang, W., Dang, Z., 2020. Influence of environmental and biological macromolecules on aggregation kinetics of nanoplastics in aquatic systems. Water Res. 186, 116316. https://doi.org/10.1016/j.watres.2020.116316.

Mao, Y., Li, H., Huangfu, X., Liu, Y., He, Q., 2020. Nanoplastics display strong stability in aqueous environments: insights from aggregation behaviour and theoretical calculations. Environ. Pollut. 258, 1–10. https://doi.org/10.1016/j.envpol.2019.113760.

Materić, D., Peacock, M., Dean, J., Futter, M., Maximov, T., Moldan, F., Röckmann, T., Holzinger, R., 2022. Presence of nanoplastics in rural and remote surface waters. Environ. Res. Lett. 17, 054036.

Oriekhova, O., Stoll, S., 2018. Heteroaggregation of nanoplastic particles in the presence of inorganic colloids and natural organic matter. Environ. Sci.: Nano 5, 792–799. https://doi.org/10.1039/c7en01119a.

Parrella, F., Brizzolara, S., Holzner, M., Mitrano, D.M., 2024. Impact of heteroaggregation between microplastics and algae on particle vertical transport. Nat. Water 2, 541–552. https://doi.org/10.1038/s44221-024-00248-z.

Pessoni, L., Veclin, C., El Hadri, H., Cugnet, C., Davranche, M., Pierson-Wickmann, A.C., Gigault, J., Grassl, B., Reynaud, S., 2019. Soap- and metal-free polystyrene latex particles as a nanoplastic model. Environ. Sci.: Nano 6, 2253–2258. https://doi.org/10.1039/c9en00384c.

Petosa, A.R., Jaisi, D.P., Quevedo, I.R., Elimelech, M., Tufenkji, N., 2010. Aggregation and deposition of engineered nanomaterials in aquatic environments: role of physicochemical interactions. Environ. Sci. Technol. 44, 6532–6549. https://doi.org/10.1021/es100598h.

Pradel, A., Catrouillet, C., Gigault, J., 2023. The environmental fate of nanoplastics: what we know and what we need to know about aggregation. NanoImpact 29, 100453. https://doi.org/10.1016/j.impact.2023.100453.

Pradel, A., Ferreres, S., Veclin, C., El Hadri, H., Gautier, M., Grassl, B., Gigault, J., 2021. Stabilization of fragmental polystyrene nanoplastic by natural organic matter: insight into mechanisms. ACS ES&T Water 1, 1198–1208. https://doi.org/10.1021/acsestwater.0c00283.

Qu, X., Hwang, Y.S., Alvarez, P.J.J., Bouchard, D., Li, Q., 2010. UV irradiation and humic acid mediate aggregation of aqueous fullerene (nC 60) nanoparticles. Environ. Sci. Technol. 44, 7821–7826. https://doi.org/10.1021/es101947f.

Sangkham, S., Faikhaw, O., Munkong, N., Sakunkoo, P., Arunlertaree, C., Chavali, M., Mousazadeh, M., Tiwari, A., 2022. A review on microplastics and nanoplastics in the environment: their occurrence, exposure routes, toxic studies, and potential effects on human health. Mar. Pollut. Bull. 181, 113832. https://doi.org/10.1016/j.marpolbul.2022.113832.

Shams, M., Alam, I., Chowdhury, I., 2020. Aggregation and stability of nanoscale plastics in aquatic environment. Water Res. 171, 115401. https://doi.org/10.1016/j.watres.2019.115401.

Shen, M., Zhang, Y., Zhu, Y., Song, B., Zeng, G., Hu, D., Wen, X., Ren, X., 2019. Recent advances in toxicological research of nanoplastics in the environment: a review. Environ. Pollut. 252, 511–521. https://doi.org/10.1016/j.envpol.2019.05.102.

Shiu, R.-F., Vazquez, C.I., Tsai, Y.-Y., Torres, G.V., Chen, C.-S., Santschi, P.H., Quigg, A., Chin, W.-C., 2020. Nano-plastics induce aquatic particulate organic matter (microgels) formation. Sci. Total Environ. 706, 135681. https://doi.org/10.1016/j.scitotenv.2019.135681.

Singh, N., Tiwari, E., Khandelwal, N., Darbha, G.K., 2019. Understanding the stability of nanoplastics in aqueous environments: effect of ionic strength, temperature, dissolved organic matter, clay, and heavy metals. Environ. Sci.: Nano 6, 2968–2976. https://doi.org/10.1039/c9en00557a.

Smith, E.J., Davison, W., Hamilton-Taylor, J., 2002. Methods for preparing synthetic freshwaters. Water Res. 36, 1286–1296. https://doi.org/10.1016/S0043-1354(01)00341-4.

Su, J., Ruan, J., Luo, D., Wang, J., Huang, Z., Yang, X., Zhang, Y., Zeng, Q., Li, Y., Huang, W., Cui, L., Chen, C., 2023. Differential photoaging effects on colored nanoplastics in aquatic environments: physicochemical properties and aggregation kinetics. Environ. Sci. Technol. https://doi.org/10.1021/acs.est.3c04808.

Sullivan, G.L., Gallardo, J.D., Jones, E.W., Hollliman, P.J., Watson, T.M., Sarp, S., 2020. Detection of trace sub-micron (nano) plastics in water samples using pyrolysis-gas chromatography time of flight mass spectrometry (PY-GCToF). Chemosphere 249, 126179. https://doi.org/10.1016/j.chemosphere.2020.126179.

Sun, H., Jiao, R., An, G., Xu, H., Wang, D., 2021a. Influence of particle size on the aggregation behavior of nanoparticles: role of structural hydration layer. J. Environ. Sci. (China) 103, 33–42. https://doi.org/10.1016/j.jes.2020.10.007.

Sun, H., Jiao, R., Wang, D., 2021b. The difference of aggregation mechanism between microplastics and nanoplastics: role of Brownian motion and structural layer force. Environ. Pollut. 268, 115942. https://doi.org/10.1016/j.envpol.2020.115942.

Sun, H., Jiao, R., Xu, H., An, G., Wang, D., 2019. The influence of particle size and concentration combined with pH on coagulation mechanisms. J. Environ. Sci. 82, 39–46. https://doi.org/10.1016/j.jes.2019.02.021.

Wang, J., Zhao, X., Wu, A., Tang, Z., Niu, L., Wu, F., Wang, F., Zhao, T., Fu, Z., 2021. Aggregation and stability of sulfate-modified polystyrene nanoplastics in synthetic and natural waters. Environ. Pollut. 268, 114240. https://doi.org/10.1016/j.envpol.2020.114240.

Wang, X., Li, Y., Zhao, J., Xia, X., Shi, X., Duan, J., Zhang, W., 2020. UV-induced aggregation of polystyrene nanoplastics: effects of radicals, surface functional groups and electrolyte. Environ. Sci.: Nano 7, 3914–3926. https://doi.org/10.1039/d0en00518e.

Wang, Y., Zhang, W., Shang, J., Shen, C., Joseph, S.D., 2019. Chemical aging changed aggregation kinetics and transport of biochar colloids. Environ. Sci. Technol. 53, 8136–8146. https://doi.org/10.1021/acs.est.9b00583.

Wu, J., Jiang, R., Lin, W., Ouyang, G., 2019. Effect of salinity and humic acid on the aggregation and toxicity of polystyrene nanoplastics with different functional groups and charges. Environ. Pollut. 245, 836–843. https://doi.org/10.1016/j.envpol.2018.11.055.

Wu, J., Ye, Q., Li, P., Sun, L., Huang, M., Liu, J., Ahmed, Z., Wu, P., 2023. The heteroaggregation behavior of nanoplastics on goethite: effects of surface functionalization and solution chemistry. Sci. Total Environ. 870, 161787. https://doi.org/10.1016/j.scitotenv.2023.161787.

Xiong, S., Cao, X., Eggleston, I., Chi, Y., Li, A., Liu, X., Zhao, J., Xing, B., 2023. Role of extracellular polymeric substances in the aggregation and biological response of micro(nano)plastics with different functional groups and sizes. J. Hazard Mater. 446, 130713. https://doi.org/10.1016/j.jhazmat.2022.130713.

Xu, J.L., Lin, X., Wang, J.J., Gowen, A.A., 2022a. A review of potential human health impacts of micro- and nanoplastics exposure. Sci. Total Environ. 851, 158111. https://doi.org/10.1016/j.scitotenv.2022.158111.

Xu, Y., Ou, Q., Jiao, M., Liu, G., Van Der Hoek, J.P., 2022b. Identification and quantification of nanoplastics in surface water and groundwater by pyrolysis gas chromatography-mass spectrometry. Environ. Sci. Technol. 56, 4988–4997. https://doi.org/10.1021/acs.est.1c07377.

Xu, Y., Ou, Q., Li, X., Wang, X., van der Hoek, J.P., Liu, G., 2022c. Combined effects of photoaging and natural organic matter on the colloidal stability of nanoplastics in aquatic environments. Water Res. 226, 119313. https://doi.org/10.1016/j.watres.2022.119313.

Xu, Y., Ou, Q., van der Hoek, J.P., Liu, G., Lompe, K.M., 2024a. Photo-oxidation of micro- and nanoplastics: physical, chemical, and biological effects in environments. Environ. Sci. Technol. 58, 991–1009. https://doi.org/10.1021/acs.est.3c07035.

Xu, Y., Ou, Q., Wang, X., van der Hoek, J.P., Liu, G., 2024b. Mass concentration and removal characteristics of microplastics and nanoplastics in a drinking water treatment plant. ACS ES&T Water. https://doi.org/10.1021/acsestwater.4c00222.

Yu, S., Li, Q., Shan, W., Hao, Z., Li, P., Liu, J., 2021. Heteroaggregation of different surface-modified polystyrene nanoparticles with model natural colloids. Sci. Total Environ. 784, 147190. https://doi.org/10.1016/j.scitotenv.2021.147190.

Yu, S., Shen, M., Li, S., Fu, Y., Zhang, D., Liu, H., Liu, J., 2019. Aggregation kinetics of different surface-modified polystyrene nanoparticles in monovalent and divalent electrolytes. Environ. Pollut. 255. https://doi.org/10.1016/j.envpol.2019.113302.

Yu, Y., Astner, A.F., Zahid, T.M., Chowdhury, I., Hayes, D.G., Flury, M., 2023. Aggregation kinetics and stability of biodegradable nanoplastics in aquatic environments: effects of UV-weathering and proteins. Water Res. 239, 120018. https://doi.org/10.1016/j.watres.2023.120018.

Zhang, F., Wang, Z., Wang, S., Fang, H., Wang, D., 2019. Aquatic behavior and toxicity of polystyrene nanoplastic particles with different functional groups: complex roles of pH, dissolved organic carbon and divalent cations. Chemosphere 228, 195–203. https://doi.org/10.1016/j.chemosphere.2019.04.115.

Zhang, Y., Su, X., Tam, N.F.Y., Lao, X., Zhong, M., Wu, Q., Lei, H., Chen, Z., Li, Z., Fu, J., 2022. An insight into aggregation kinetics of polystyrene nanoplastics interaction with metal cations. Chinese Chem. Lett. 33, 5213–5217. https://doi.org/10.1016/j.cclet.2022.01.056.

Zhu, S., Mo, Y., Luo, W., Xiao, Z., Jin, C., Qiu, R., 2022. Aqueous aggregation and deposition kinetics of fresh and carboxyl-modified nanoplastics in the presence of divalent heavy metals. Water Res. 222, 118877. https://doi.org/10.1016/j.watres.2022.118877.